Science & Technology Development Journal – Engineering and Technology 2025, ():1-15

Open Access Full Text Article

Research Article

A passivity-based neural control using genetic algorithm for a DC-DC boost power converter

Minh Ngoc Huynh[1,2], Hoai Nghia Duong[3,*], Vinh Hao Nguyen[1]

ABSTRACT

In this paper, a passivity – based neural control using genetic algorithm for a DC-DC boost power converter is proposed. The output of a DC-DC boost power converter is an inductor current. The control input is the duty ratio. Using a co-ordinate transformation of state variables and control input, a DC-DC boost power converter is passive. A new plant is zero-state observable and the equilibrium point at origin of this plant is asymptotically stable. A neural network performs a passivity - based control law. The goal is that the capacitor voltage is equal to the desired voltage. The neural network has three layers: the input layer, the hidden layer and the output layer. The activation function of the hidden layer is tangent-hyperbolic and the activation of the output layer is linear. The weights of neural network are also adjusted optimally by genetic algorithm using decimal encoder. Simulation results are done with Simulink in MATLAB. Simulation results of the passivity-based neural control without using genetic algorithm show that the capacitor voltage is kept at the desired voltage when the desired voltage, the input voltage, and the load resistor vary. The results of passivity-based neural control using genetic algorithm show that the capacitor voltage is kept at the desired value when the input voltage and the load resistor change. Further, the simulation results of the passivity – based neural control using genetic algorithm have better performance such as shorter settling time and smaller value of IAE (integral absolute error of the desired voltage and the capacitor voltage) than the neural control when the input voltage varies. Finally, simulation results show that the passivity-based neural control using genetic algorithm has shorter settling time than the neural control when the load resistor changes.

Key words: DC-DC boost power converter, neural control, passivity – based control, genetic algorithm

[1]*Ho Chi Minh City University of Technology (HCMUT), Vietnam National University Ho Chi Minh City, Vietnam*

[2]*Industrilal University of Ho Chi Minh City, Vietnam*

[3]*Eastern International University, Vietnam*

Correspondence

Hoai Nghia Duong, Eastern International University, Vietnam

Email: nghia.duong@eiu.edu.vn

History

- Received: 16-1-2024
- Revised: 31-8-2024
- Accepted: 22-10-2024
- Published Online:

DOI :

Check for updates

INTRODUCTION

The neural control and the passivity-based control have been investigated by many researchers. Ortega et al.[1] presented the passivity-based control of DC-DC boost converter and buck converter, the sliding mode control and the adaptive control for DC-DC power converter. W. He et al.[2] presented the passivity-based control of DC-DC boost power converter under time-varying disturbances via generalized proportional integral observer. Cisneros et al.[3] presented the passivity-based control of the bilinear systems and its applications to the boost and modular multilevel converters. The sliding mode control and the passivity-based control were presented by Hoai Nghia Duong[4]. Khalil[5] presented the Lyapunov stable theory, a passivation and the passivity-based control of a two-degree of freedom robot. M. H. Huynh, H. N. Duong and V. H. Nguyen[6] presented the control system based on passivity-based control for a bicycle robot.

T. Hayakawa et al.[7] described the passivity-based adaptive output feedback control using neural network for nonlinear nonnegative dynamical systems. W. Li et al.[8] presented the passivity-based distributed tracking control problem of networked agents in the presence of uncertainty and external disturbance. M. Norgaard et al.[9] presented the multilayer perceptron network and applications to identification of nonlinear systems, the inverse control, and the internal model control of nonlinear systems. Duc Minh Nguyen et al.[10] described the control of the inverted pendulum system using neural networks. D. Muthirayan and P. P. Khargonekar[11] presented a neural adaptive control for a continuous-time system. G. Escobar et al.[12] presented an experimental comparison of several nonlinear controllers such as input-output linearization, sliding mode control, and passivity-based control for DC-DC boost power converter. M. A. Hassan et al.[13] presented the passivity-based control combined with adaptive control of DC-DC buck converter with constant power loads in DC microgrid systems.

Further, genetic algorithm was described by M. Mitchell[14]. K. S. Tang et al.[15] presented an optimiza-

Cite this article : Huynh M N, Duong H N, Nguyen V H. **A passivity-based neural control using genetic algorithm for a DC-DC boost power converter**. *Sci. Tech. Dev. J. – Engineering and Technology* 2025; ():1-15.

tion of feedforward neural networks of which topology and weights were adjusted optimally by genetic algorithm. The neural networks integrated adaptive backstepping control of DC-DC boost converter were presented by T. K. Nizami and A. Chakravarty [16]. J. Aguila-Leon et al. [17] presented an optimal PID parameters tuning for a DC-DC boost converter. M. Mohammedi et al. [18] described the fuzzy logic and passivity-based controller applied to electric vehicle using fuel cell and supercapacitors hybrid source. A passivity-based control using genetic algorithm was proposed by M. N. Huynh, H. N. Duong and V. H. Nguyen [19]. The advantage of the passivity-based control is the asymptotical stability of the equilibrium point at origin of the plant. The passivity-based control combined with sliding mode control for a DC-DC boost power converter was presented by Minh Ngoc Huynh, Hoai Nghia Duong and Vinh Hao Nguyen [20]. J. Wu and Y. Lu [21] described the adaptive backtepping sliding mode control for DC-DC boost converter with constant power load.

In this paper, a passivity – based neural control using genetic algorithm of a DC-DC boost power converter is proposed. The weights of neural network are adjusted optimally by genetic algorithm using decimal encoder. Simulation results are done with Simulink in MATLAB.

The paper is organized as follows. The introduction is presented in section 1. The dynamical model of a DC-DC boost power converter, the passivity-based method and the passivity property of a DC-DC boost power converter are presented in section 2. Section 3 presents the passivity-based neural network control and the tuning the weights of neural network using genetic algorithm. The simulation results and discussions are described in section 4. Finally, conclusions are presented in section 5.

PRELIMINARY AND RESEARCH METHOD

Dynamical model of a DC-DC boost power converter

A DC-DC boost power converter is described in Figure 1.

When the switch is at 2, the inductor current i increases and stores energy in the inductor L. When the switch is at 1, the current i decreases and the energy, which is from the input voltage E and the inductor L, stores in the capacitor C (and supplies in the load resistor R). The output voltage of DC-DC boost power converter is higher than the input voltage E.

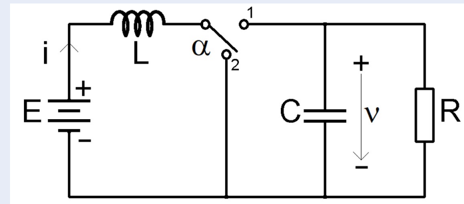

Figure 1: A DC-DC boost power converter.

Let $x_1 = i$, $x_2 = v$. x_1 is the inductor current i, and x2 is the capacitor voltage v. A state-space model of a DC-DC boost power converter is as follows by Ortega [1]

$$\begin{cases} \dot{x}_1 = -(1-\alpha)\dfrac{1}{L}x_2\dfrac{E}{L} \\ \dot{x}_2 = (1-\alpha)\dfrac{1}{C}x_1 - \dfrac{1}{RC}x_2 \end{cases} \tag{1}$$

The output signal is x_1. The switch variable a is equal to 1 when there is $0 < t < T_1$; a is equal to 0 when there is $T_1 < t < T$. T is constant.

Ortega used an average model [1] to design the controllers as follows

$$\begin{cases} \dot{x}_1 = -(1-u)\dfrac{1}{L}x_2\dfrac{E}{L} \\ \dot{x}_2 = (1-u)\dfrac{1}{C}x_1 - \dfrac{1}{RC}x_2 \end{cases} \tag{2}$$

where x_1 and x_2 are the corresponding averaged variables. The control signal u is the duty ratio $u = \frac{T_1}{T}$. The control signal u is continuous and $0 < u < 1$. Let Vd be the desired value of the capacitor v. The operating point of the system (2) is

$$x_{10} = \frac{V_d^2}{ER};\ x_{20} = V_d;\ u_0 = 1 - \frac{E}{V_d} \tag{3}$$

With E= 15 (V), R= 30 (Ω), V_d = 20 (V), we have: $x_{i0} = 0.888$; $x_{20} = 20$; $u_0 = 0.25$

Our goal is to regulate the capacitor voltage v to the desired value V_d while E and R can vary.

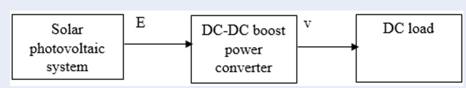

Figure 2: Application of a DC-DC boost power converter.

Practical application: the DC-DC boost power converter is used in a solar photovoltaic system (PV). The photovoltaic system and DC load cannot connect directly. The DC-DC boost power converter is needed. The application of a DC-DC boost power converter is illustrated in Figure 2.

Passivity-based control method

Consider the dynamical system in the following form:

$$\begin{cases} \dot{x} = f(x,u) \\ y = h(x) \end{cases} \tag{4}$$

where f is locally Lipschitz; h is continuous; f(0,0)=0, h(0)=0.

The plant is passive if there exists a continuously differentiable positive semidefinite function V(x), which is called the storage function, such that

$$u^T y \geq \dot{V} = \frac{\partial V}{\partial x} f(x,u)\ \forall (x,u)$$

Consider the plant (4) with u=0. The plant is zero-state observable if $y \equiv 0$ then $x \equiv 0$.

Property[4]: Consider the plant (4). If the plant satisfies the following conditions:

i) Passive with a storage function V(x) which is positive semidefinite.

ii) Zero-state observable.

iii) $V(x) \to \infty$ as $x \to \infty$.

Then with the feedback control law $u = -\varphi(y)$ with $\varphi(0) = 0$; $y^T \varphi(y) > 0\, \forall y \neq 0$, the origin achieves the global asymptotic stability.

Passivity of DC-DC boost power converter

We change the variables as follows

$$\begin{aligned} \tilde{x}_1 &= x_1 - x_{10} = x_1 - \frac{V_d^2}{ER} \\ \tilde{x}_2 &= x_2 - x_{10} = x_1 - V_d \\ \tilde{u} &= u - u_0 = u - \left(1 - \frac{E}{V_d}\right) \end{aligned} \tag{5}$$

Note that $\dot{\tilde{x}}_1 = \dot{x}_1$; $\dot{\tilde{x}}_2 = \dot{x}_2 = [\tilde{x}_1, \tilde{x}_2]^T$

Insert (5) into (2), we obtain the state-space equation of the plant

$$\begin{cases} \dot{\tilde{x}}_1 = \dfrac{\tilde{u}}{L}(\tilde{x}_2 + V_d) - \dfrac{E}{LV_d}\tilde{x}_2 \\ \dot{\tilde{x}}_2 = -\dfrac{\tilde{u}}{C}\left(\tilde{x}_1 + \dfrac{V_d^2}{ER}\right) + \dfrac{E}{CV_d}\tilde{x}_1 - \dfrac{1}{RC}\tilde{x}_2 \end{cases} \tag{6}$$

The storage function V is chosen as follows

$$V(\tilde{x}) = \frac{1}{2}L\tilde{x}_1^2 + \frac{1}{2}C\tilde{x}_2^2 \tag{7}$$

The function V is positive definite because $V(0,0) = 0$; $V(\tilde{x}_1, \tilde{x}_2) > 0\, \forall \tilde{x}_1 \neq 0,\ \tilde{x}_2 \neq 0$. The derivative of V is as follows

$$\dot{V} = L\tilde{x}_1\dot{\tilde{x}}_1 + L\tilde{x}_2\dot{\tilde{x}}_2$$

Insert (6) into $\dot{V}$, we have

$$\begin{aligned} \dot{V} &= \left(L\tilde{x}_1\dot{\tilde{x}}_1 + L\tilde{x}_2\dot{\tilde{x}}_2\right) \\ &= L\tilde{x}_1\left[\frac{\tilde{u}}{L}(\tilde{x}_2 + V_d) - \frac{E}{LV_d}\tilde{x}_2\right] + L\tilde{x}_2\dot{\tilde{x}}_2 + \\ & L\tilde{x}_2\left[-\frac{\tilde{u}}{C}\left(\tilde{x}_1 + \frac{V_d^2}{ER}\right) + \frac{E}{CV_d}\tilde{x}_1 - \frac{1}{RC}\tilde{x}_2\right] \\ &= (\tilde{x}_1\tilde{u}\tilde{x}_2 + V_d\tilde{x}_1\tilde{u} - \frac{E}{V_d}\tilde{x}_2\tilde{x}_1 - \tilde{x}_1\tilde{u}\tilde{x}_2 - \\ & \tilde{x}_2\tilde{u}\frac{V_d^2}{ER} + \frac{E}{V_d}\tilde{x}_1\tilde{x}_2 - \frac{1}{R}\tilde{x}_2^2) \\ & \Rightarrow \dot{V} = V_d\tilde{x}_1\tilde{u} - \frac{V_d^2}{ER}\tilde{x}_2\tilde{u} - \frac{1}{R}\tilde{x}_2^2 \\ & \Rightarrow \dot{V} = (x_{20}\tilde{x}_1 - x_{10}\tilde{x}_2)\,\tilde{u} - \frac{1}{R}\tilde{x}_2^2 \end{aligned} \tag{8}$$

The plant (6), which has the input $\tilde{u}$ and the output $\tilde{y}$, is passive because $\tilde{y}\tilde{u} = \dot{V} + \frac{1}{R}\tilde{x}_2^2 \Rightarrow \tilde{y}\tilde{u} \geq \dot{V}$. .

The plant (6) is zero-state observable because $\tilde{u} = 0, \tilde{y} = 0 \Rightarrow \tilde{x}_1 \equiv 0 \Rightarrow \tilde{x}_2 \equiv 0 \Rightarrow \tilde{x} \equiv 0$..

PASSIVITY-BASED NEURAL CONTROL

Passivity-based control

The passivity-based control is constructed as follows[19].

According to the property[4], the control law stabilizes the equilibrium point at origin of (6):

$\tilde{u} = -\varphi(\tilde{y})$ with $\varphi(0) = 0$; $\tilde{y}\varphi(\tilde{y}) > 0 \forall \tilde{y} \neq 0$ (9)

We can choose

$$\varphi(\tilde{y}) = a_1\tilde{y} + a_2\tilde{y}^3 + a_3\tilde{y}^5 \tag{10}$$

The passivity-based control law is

$$\begin{aligned} u = -a_1 &\left[V_d\left(x_1 - \frac{V_d^2}{ER}\right) - \frac{V_d^2}{ER}(X_2 - V_d)\right]^5 \\ &+ \left(1 - \frac{E}{V_d}\right) \end{aligned} \tag{11}$$

Passivity-based neural control

Now we construct a neural network which performs the passivity-based control law (11). The neural network has three inputs: in_1, in_2, in_3 and output u. The hidden layer has three neurons and its activation is tangent hyperbolic. The output layer has one neuron and its activation is linear. The structure of the neural network is described in Figure 3.

$$\begin{aligned} in_1 &= -\left[V_d\left(x_1 - \frac{V_d^2}{ER}\right) - \frac{V_d^2}{ER}(X_2 - V_d)\right]; \\ in_2 &= -\left[V_d\left(x_1 - \frac{V_d^2}{ER}\right) - \frac{V_d^2}{ER}(X_2 - V_d)\right]^3; \\ in_3 &= -\left[V_d\left(x_1 - \frac{V_d^2}{ER}\right) - \frac{V_d^2}{ER}(X_2 - V_d)\right]^5. \end{aligned} \tag{12}$$

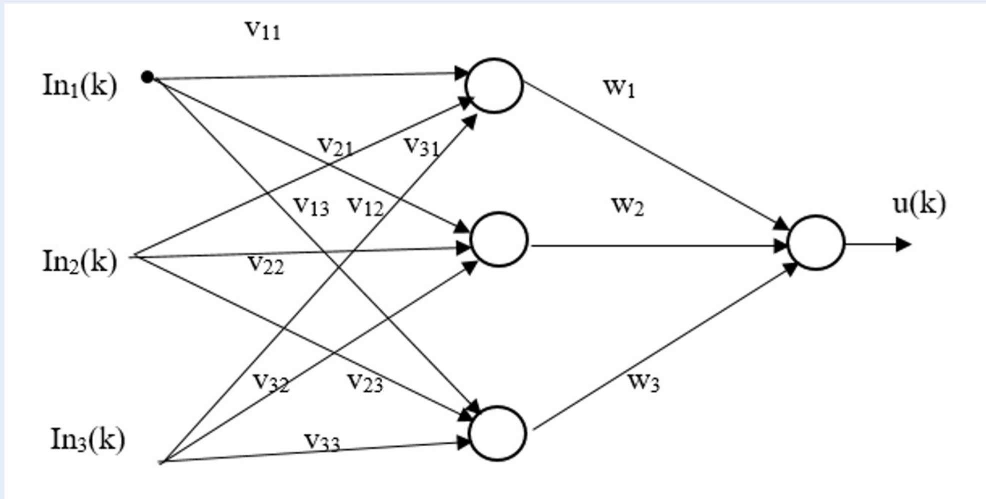

Figure 3: The structure of neural network.

The output of the neural network is u(k).

Algorithm is as follows

Step 1: Setup the initial parameters of DC-DC boost power converter.

Step 2: Construct the simulation scheme of the neural control for a DC-DC boost power converter and collect data for genetic algorithm to adjust the weights of the neural network.

Step 3: Adjust the weights of the neural controller using genetic algorithm.

The structure of the neural control for a DC-DC boost power converter is described in Figure 4.

Tuning the weights of neural network using genetic algorithm

The plant (2) is controlled by the neural control. V_{ij} is the weights of the hidden layer with i=1,2,3; j=1,2,3. W_k is the weights of the output layer with k=1,2,3. The parameters v_{11}, v_{21}, v_{31}, v_{12}, v_{22}, v_{32}, v_{13}, v_{23}, v_{33}, w_1, w_2 and w_3 are determined such that the function J is minimized with $q_1>0$, $q_2>0$.

$$J=\int_0^{+\infty}\left(q_1\tilde{x}_1^2(t)+q_2\tilde{x}_2^2(t)+\tilde{u}^2(t)\right)dt \quad (14)$$

We use genetic algorithm with decimal encoder. The selection is a linear ranking. The crossover is two-point. Crossover probability is equal to 0.9. The mutation is uniform mutation with many points. Mutation probability is equal to 0.1. The parameters θ is encoded into the chromosome which has twelve gene segments indicated by v_{11}, v_{21}, v_{31}, v_{12}, v_{22}, v_{32}, v_{13}, v_{23}, v_{33}, w_1, w_2 and w_3 in Table 1. The value range is: $0\le v_{11}\le 1$, $0\le v_{21}\le 1$, $0\le v_{31}\le 1$, $0\le v_{12}\le 1$, $0\le v_{22}\le 1$, $0\le v_{32}\le 1$, $0\le v_{13}\le 1$, $0\le v_{23}\le 1$, $0\le v_{33}\le 1$, $0\le w_1\le 1$, $0\le w_2\le 1$, $0\le w_3\le 1$. The maximum generation is equal to 100. The population size is equal to 30. The exact value ε is equal to 10^6. The discrete version of the J is as follows

$$\begin{aligned}J&=\sum_{k=1}^{N}\left(q_1\tilde{x}_1^2(k)+q_2\tilde{x}_2^2(k)+\tilde{u}^2(k)\right)\\&=\sum_{k=1}^{N}[q_1\left(x_1(k)-\frac{V_d^2}{E\times R}\right)^2+\\&q_2\left(x_2(k)-V_d\right)^2+\left(u(k)-\left(1-\frac{E}{V_d}\right)\right)^2]\end{aligned} \quad (15)$$

We have a fitness function $\frac{1}{J+\varepsilon}$.

x_{1n}(k) and x_{2n}(k) are the state variables $\tilde{x}_1$ and $\tilde{x}_2$ at k^{th} sample. u_n(k) is the control input $\tilde{u}$ at k^{th} sample.

SIMULATION RESULTS AND DISCUSSIONS

The parameters of the circuits are described in Table 2. The input voltage E varies from 12 (V) to 16.5 (V). The resistor R varies from 15 (Ω) to 40 (Ω). The initial weights of neural network are: v_{11}=0.5, v_{21}=0.5, v_{31}=0.5, v_{12}=0.5, v_{22}=0.5, v_{32}=0.5, v_{13}=0.5, v_{23}=0.5, v_{33}=0.5, w_1=0.2, w_2=0.2, w_3=0.2. Initially, x_1 (0) = 0 A, x_2(0) =0 V.

Passivity-based neural control withour using genetic algorithm

The simulation time is set to be 45 ms.

Response to the variations of E: At the beginning of the simulation, the input voltage E is set to be 15 (V). At t= 15 ms, E is increased to 16.5 (V) and at t=30 ms, E is decreased to 15 (V). The results are described in Figure 5 and Table 3.

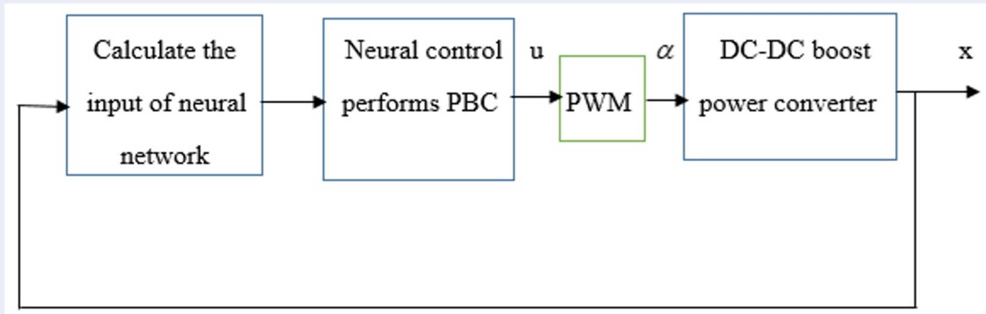

Figure 4: The structure of the neural control for a DC-DC boost power converter.

Table 1: The parameters v_{11}, v_{21}, v_{31}, v_{12}, v_{22}, v_{32}, v_{13}, v_{23}, v_{33}, w_1, w_2 and w_3.

Parameters	v11	v21	v31	v12	v22	v32
Gene segment	1	2	3	4	5	6
Parameters	v13	v23	v33	w1	w2	w3
Gene segment	7	8	9	10	11	12

Table 2: The parameters of the DC-DC boost power converter.

Parameters	Physical Meaning	Value
C	Capacitor	68 (μF)
L	Inductor	0.02 (H)
E	Input voltage	15 (V)
R	Load resistor	30 Ω
Vd	Desired voltage	20 (V)

Figure 5 shows the current i, the control input u, the capacitor voltage v, and the input voltage E when the system is controlled by the passivity-based NC without using GA and the input voltage E varies. Figure 5 shows that at t=15 ms, when E is increased to 16.5 V, the inductor current i is equal to 0.79 A. At t=30 ms, when E is decreased to 15 V, the inductor current i is equal to 0.888 A. The settling time is equal to 3 ms. Figure 5 shows that at t=15 ms, when E is increased to 16.5 V, the capacitor voltage v has the value $\triangle V = |V_d - x_2|$ (V) of 0.80759 V. The settling time is equal to 3.3 ms and v is equal to 20 V. At t=30 ms, when E is decreased to 15 V, the capacitor voltage v has $\triangle V$ (V) of 1.0436 V and v is equal to 20 V. The settling time is equal to 3.3 ms. The value of IAE (integral absolute error (IAE) between V_d and x_2) is 0.0412.

$IAE = \int_0^{+\infty} |V_d - x_2$

Response to the variations of R: At the beginning of the simulation, the load resistor R is set to be 30 (Ω). At t=15 ms, R is increased to 40 (Ω). At t=30 ms, R is decreased to 30 (Ω). The results are described in Figure 6 and Table 4.

Figure 6 is the simulation results of passivity-based NC without GA when R changes. Figure 6 shows the current i, the control input u, the capacitor voltage v and the load resistor R. Figure 6 shows that at t=15 ms, when R is increased to 40 Ω, the inductor current i is equal to 0.667 A. At t=30 ms, when R is decreased to 30 Ω, the inductor current i is equal to 0.888 A. The settling time is equal to 3.1 ms. Figure 6 shows that at t=15 ms, when R is increased to 40 Ω, the capacitor voltage v has the value $\triangle V$ (V) of 2.10345 V. The settling time is equal to 9.2 ms and v is equal to 20 V. At t=30 ms, when R is deceased to 30 Ω, the capacitor voltage v has $\triangle V$ (V) of 1.847 V and v is equal to 20 V. The settling time is equal to 9.2 ms. The value of IAE is 0.0478.

Response to the variations of V_d: At the beginning of the simulation, the desired voltage V_d is set to be 20(V). At t=15 ms, V_d is decreased to 17 (V). At t=30 ms, V_d is increased to 20 (V). The results are described

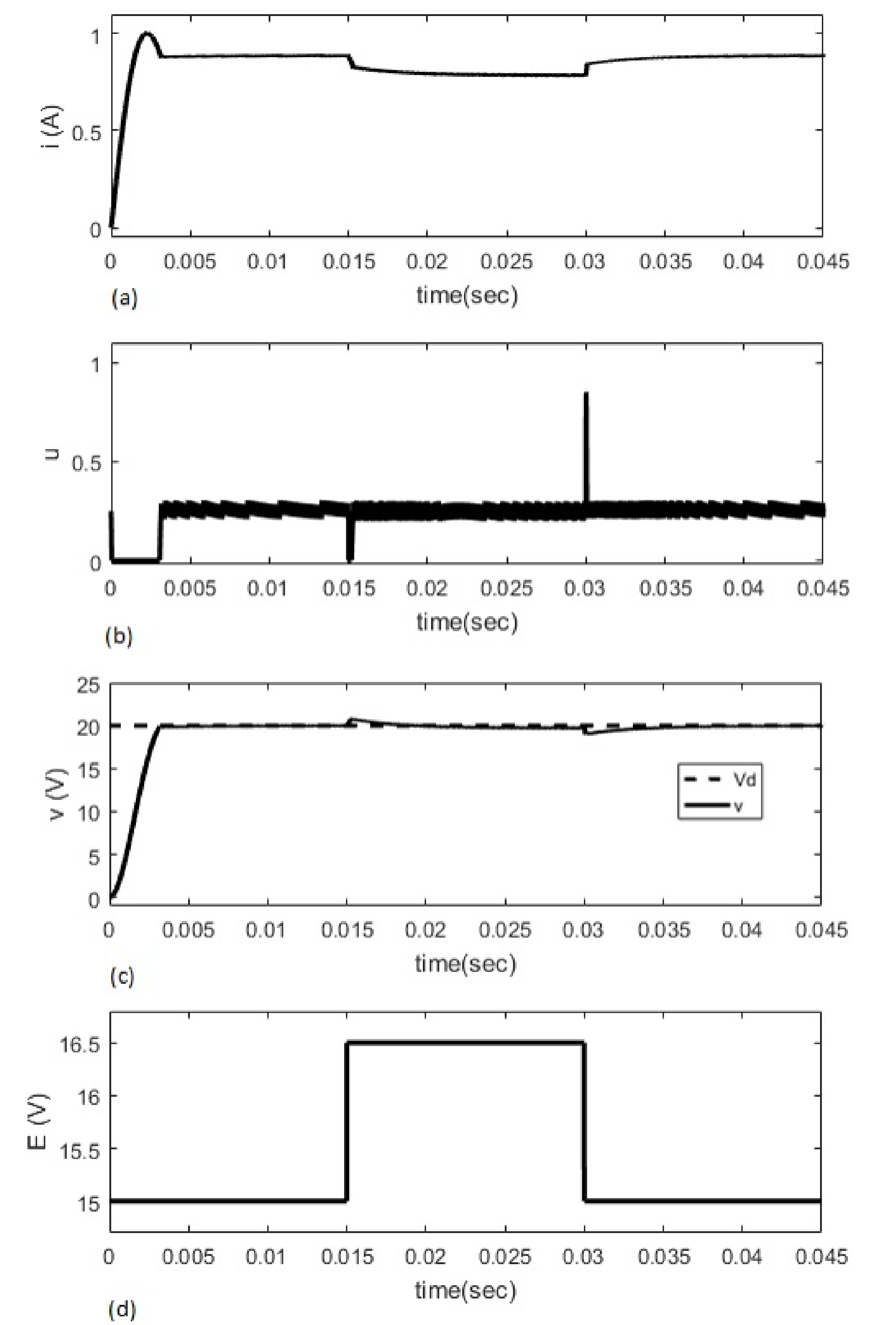

Figure 5: The results of the passivity-based NC without GA when E changes: (a) the inductor current i, (b) the control input u, (c) the capacitor voltage v, and (d) the input voltage E.

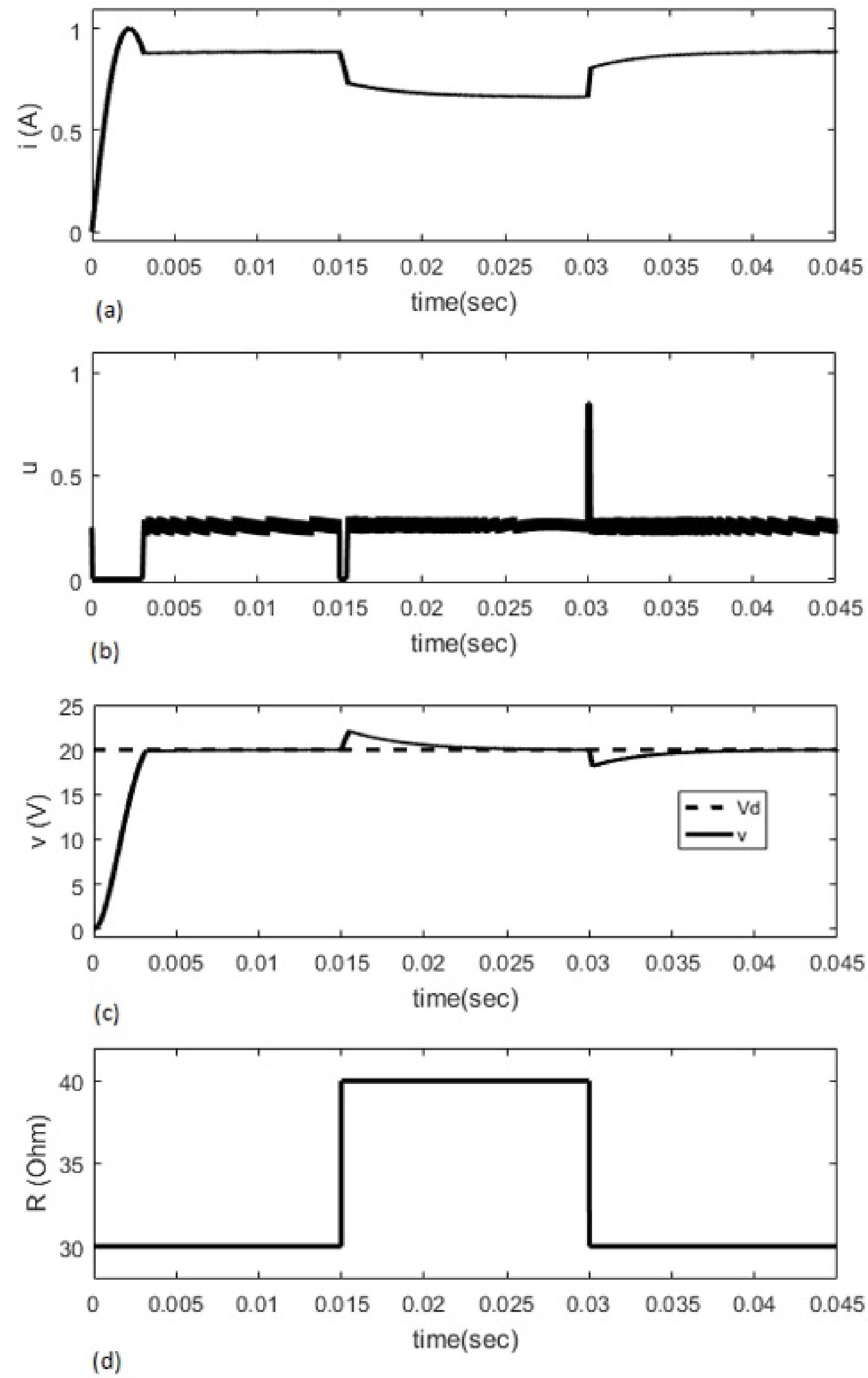

Figure 6: The results of the passivity-based NC without GA when R changes: (a) the inductor current i, (b) the control input u, (c) the capacitor voltage v, and (d) the load resistor R.

Table 3: The capacitor voltage v when E varies.

Increasing (+1.5V)		Decreasing (-1.5V)	
$\triangle V = \lvert V_d - x_2 \rvert$ (V)	Settling time ts t_s (ms)	$\triangle V$ (V)	Settling time t_s (ms)
0.80759	3.3 ms	1.0436	3.3 ms

Table 4: The capacitor voltage v when R varies.

Increasing (+10 Ω)		Decreasing (-10 Ω)	
$\triangle V$ (V)	t_s (ms)	$\triangle V$ (V)	t_s (ms)
2.10345	9.2 ms	1.847	9.2 ms

in Figure 7 and Table 5.

Figure 7 is the simulation results of passivity-based NC without GA when V_d changes. Figure 7 shows the current i, the control input u, the capacitor voltage v and the desired voltage V_d. Figure 7 shows that at t=15 ms, when V_d is decreased to 17 V, the capacitor voltage v has the value $\triangle V$ (V) of 0.91785 V. The capacitor voltage v is equal to 17 V and the settling time is equal to 3 ms. At t=30 ms, when V_d is increased to 20 V, the capacitor voltage v has the value $\triangle V$ (V) of 1.523 V, and v is equal to 20 V. The value of IAE is 0.0622.

Passivity-based neural control using genetic algorithm

The simulation time is set to be 45 ms. The results of passivity-based NC before using GA are used to collect data for tuning the parameters using GA.

The initial weights of neural network are: v_{11}=0.5, v_{21}=0.5, v_{31}=0.5, v_{12}=0.5, v_{22}=0.5, v_{32}=0.5, v_{13}=0.5, v_{23}=0.5, v_{33}=0.5, w_1=0.2, w_2=0.2, w_3=0.2.

Response to the variations of E: At the beginning of the simulation, the input voltage E is set to be 15 (V). At t= 15 ms, E is increased to 16.5 (V) and at t=30 ms, E is decreased to 15 (V).

The results of the passivity-based neural control using GA, with q_1=1, q_2=1, are presented when E changes. The results at generation 0 are: v_{110}=0.6787, v_{210}=0.7577, v_{310}=0.7431, v_{120}=0.3922, v_{220}=0.6555, v_{320}=0.1712, v_{130}=0.706, v_{230}=0.0318, v_{330}=0.2769, w_{10}=0.0462, w_{20}=0.0971, w_{30}=0.8235, $J_0 = 49960$. The optimal results after tuning the parameters using GA are as follows: v_{11}=0.694, v_{21}=0.015, v_{31}=0.743, v_{12}=0.034, v_{22}=0.438, v_{32}=0.381, v_{13}=0.761, v_{23}=0.431, v_{33}=0.015, w_1=0.045, w_2=0.09, w_3=0.646, J=49858. Stop at generation 51. The best chromosome is 1. The cost function is illustrated in Figure 8. When E changes, the results of the passivity-based neural control using genetic algorithm is illustrated in Figure 9 and Table 6.

Figure 9 shows the current i, the control input u, the capacitor voltage v, and the input voltage E when the system is controlled by passivity-based NC using GA and the input voltage E varies. Figure 9 shows that at t=15 ms, when E is increased to 16.5 V, the inductor current i is equal to 0.802 A. At t=30 ms, when E is decreased to 15 V, the inductor current i is equal to 0.893 A. The settling time is equal to 2.9 ms. Figure 9 shows that at t=15 ms, when E is increased to 16.5 V, the capacitor voltage v has the value $\triangle V = \lvert V_d - x_2 \rvert$ (V) of 0.79965 V. The settling time is equal to 2.9 ms and v is equal to 20 V. At t=30 ms, when E is decreased to 15 V, the capacitor voltage v has $\triangle V$ (V) of 0.8723 V and v is equal to 20 V. The settling time is equal to 2.9 ms. The value of IAE is 0.0391.

Genetic algorithm is integrated into a neural controller and adjusts optimally the weights of the neural network such as v_{11}, v_{21}, v_{31}, v_{12}, v_{22}, v_{32}, v_{13}, v_{23}, v_{33}, w_1, w_2 and w_3. The value of q_1 has influence to the inductor current i and decreases the settling time, 2.9 ms. The value of q_2 has influence to the capacitor voltage v and decreases the settling time, 2.9 ms.

The results show that compared with the neural control without GA, the proposed passivity-based neural control using GA has shorter settling time and smaller value of IAE when E changes. Moreover, the passivity-based NC using GA has smaller value of $\triangle V$. The comparison results are described in Figure 10 and Table 6.

Response to the variations of R: At the beginning of the simulation, the load resistor R is set to be 30 (Ω). At t=15 ms, R is increased to 40 (Ω). At t=30 ms, R is decreased to 30 (Ω).

The results of the passivity-based neural control using GA, with q_1=1, q_2=1, are presented when R changes. The results at generation 0 are: v_{110}=0.6563, v_{210}=0.8349, v_{310}=0.6399, v_{120}=0.3271, v_{220}=0.275, v_{320}=0.2164, v_{130}=0.2794, v_{230}=0.2528, v_{330}=0.711, w_{10}=0.0821, w_{20}=0.2998, w_{30}=0.1112, $J_0 = 50916$. The optimal results after tuning the parameters

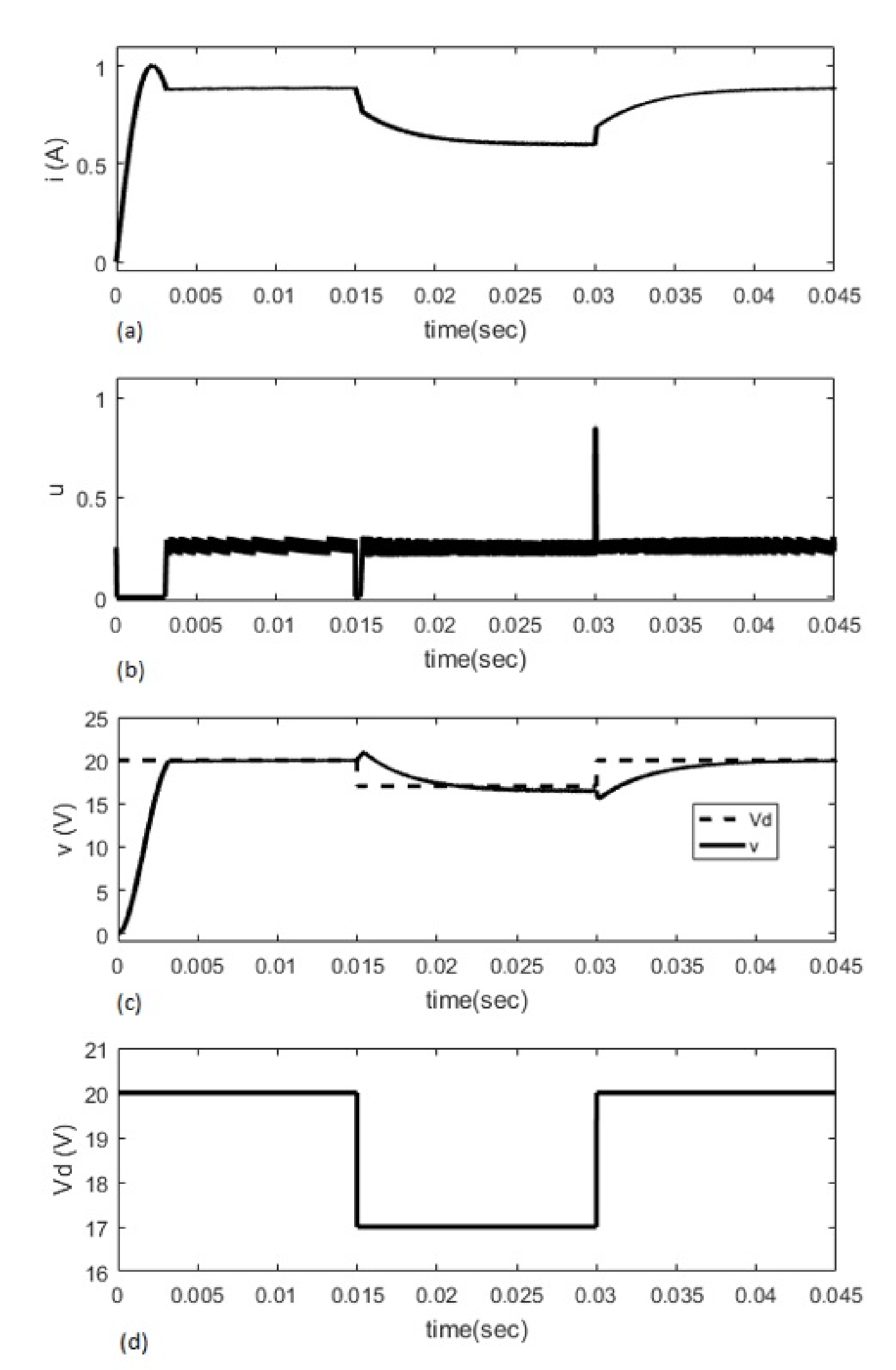

Figure 7: The results of the passivity-based NC without GA when V_d changes: (a) the inductor current i, (b) the control input u, (c) the capacitor voltage v, and (d) the desired voltage V_d.

Table 5: The capacitor voltage v when V_d varies.

Decreasing (-3 V)		Increasing (+3 V)	
$\triangle V$ (V)	t_s (ms)	$\triangle V$ (V)	t_s (ms)
0.91786	3 ms	1.523	3 ms

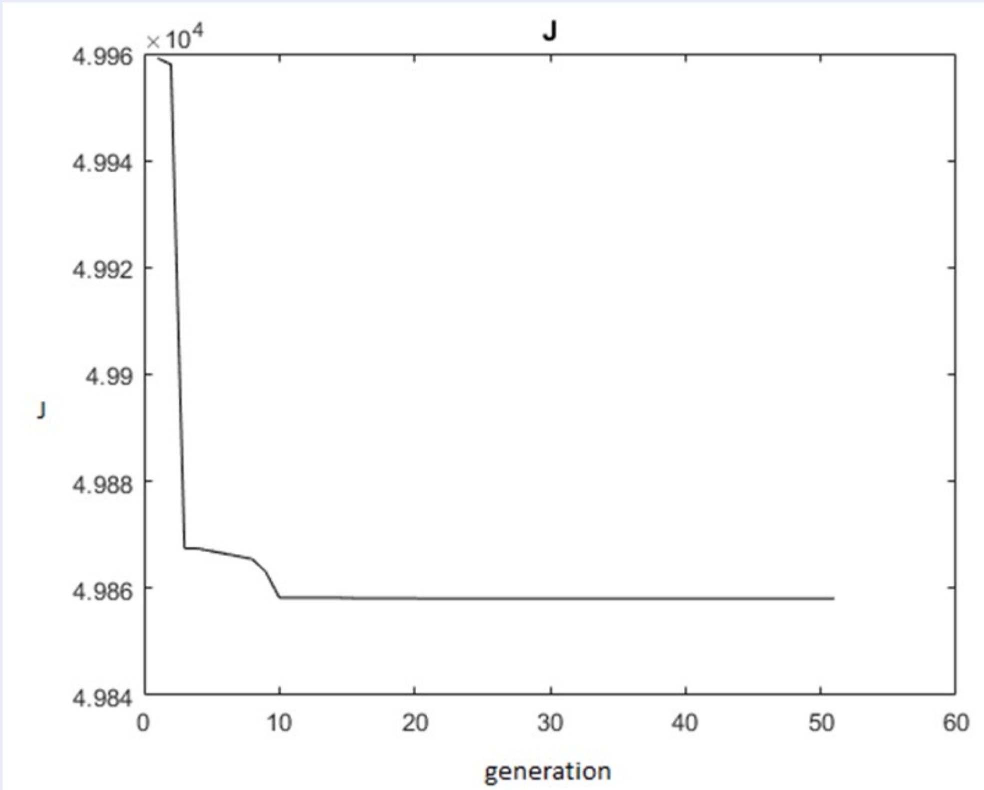

Figure 8: The cost function J of the passivity-based NC using GA with q_1=1, q_2=1 when E varies.

Table 6: The capacitor voltage v of the NC without GA and the passivity-based NC using GA with q_1=1, q_2=1 when E varies.

Controller	Increasing (+1.5V)		Decreasing (-1.5V)		IAE
	$\triangle V$ (V)	ts (ms)	$\triangle V$ (V)	ts (ms)	
NC without GA	0.80759	3.3	1.0436	3.3	0.0412
Passivity-based NC using GA with q_1=1, q_2=1	0.79965	2.9	0.8723	2.9	0.0391

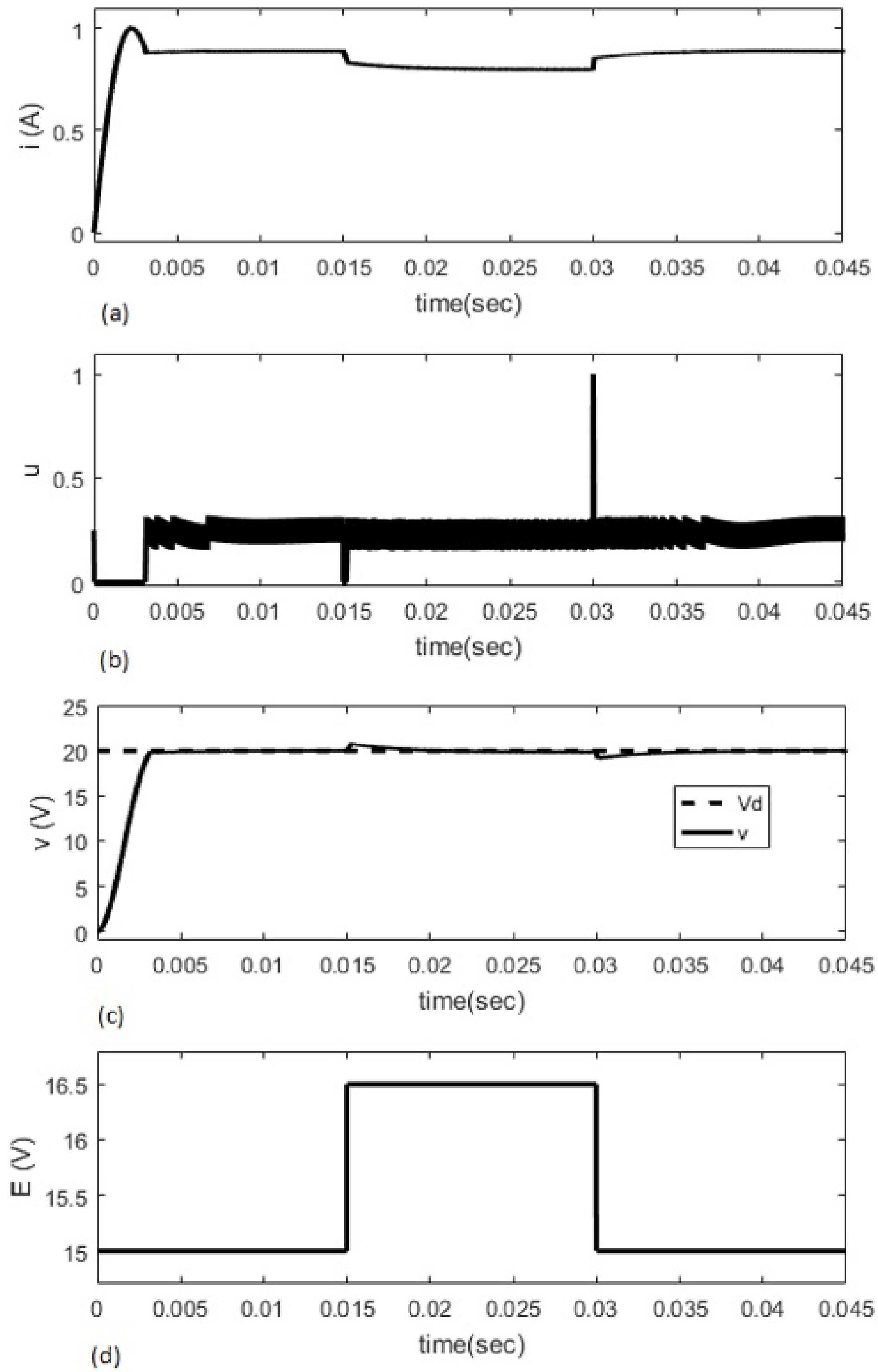

Figure 9: The results of the passivity-based NC using GA with q_1=1, q_2=1 when E changes: (a) the inductor current i, (b) the control input u, (c) the capacitor voltage v and (d) E.

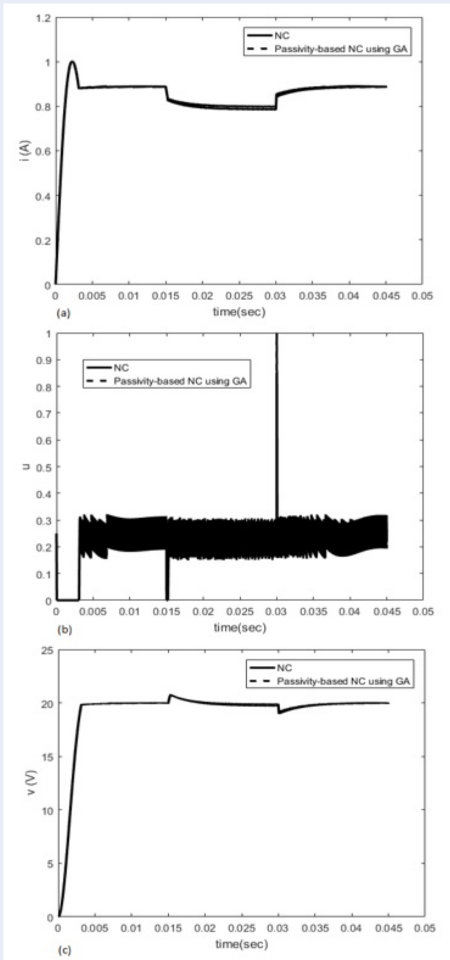

Figure 10: The results of NC without GA (continuous line) and the passivity-based NC using GA (discrete line) when E changes: (a) the inductor current i, (b) the control input u, and (c) the capacitor voltage v with q_1=1, q_2=1.

using GA are as follows: v_{11}=0.646, v_{21}=0.633, v_{31}=0.639, v_{12}=0.394, v_{22}=0.736, v_{32}=0.326, v_{13}=0.52, v_{23}=0.077, v_{33}=0.21, w_1=0.05, w_2=0.299, w_3=0.111, J=50910. Stop at generation 51. The best chromosome is 1. The cost function is illustrated in Figure 11. When R changes, the results of the passivity-based neural control using genetic algorithm is illustrated in Figure 12 and Table 7.

Figure 12 is the simulation results of passivity-based NC without GA when R changes. Figure 12 shows the current i, the control input u, the capacitor voltage v and the load resistor R. Figure 12 shows that at t=15 ms, when R is increased to 40 Ω, the inductor current i is equal to 0.665 A. At t=30 ms, when R is decreased to 30 Ω, the inductor current i is equal to 0.885 A. The settling time is equal to 3 ms. Figure 12 shows that

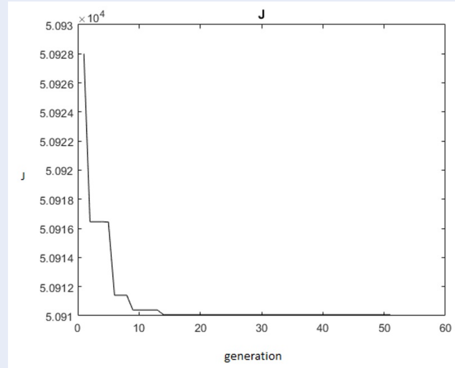

Figure 11: The cost function J of the passivity-based NC using GA with q_1=1, q_2=1 when R varies.

at t=15 ms, when R is increased to 40 Ω, the capacitor voltage v has the value $\triangle V$ (V) of 2.022 V. The settling time is equal to 2.8 ms and v is equal to 20 V. At t=30 ms, when R is deceased to 30 Ω, the capacitor voltage v has $\triangle V$ (V) of 1.873 V and v is equal to 20 V. The settling time is equal to 2.8 ms. The value of IAE is 0.0482.

Genetic algorithm is integrated into a neural controller and adjusts optimally the weights of the neural network such as v_{11}, v_{21}, v_{31}, v_{12}, v_{22}, v_{32}, v_{13}, v_{23}, v_{33}, w_1, w_2 and w_3. The value of q_1 has influence to the inductor current i and decreases the settling time, 3 ms. The value of q_2 has influence to the capacitor voltage v and decreases the settling time, 2.8 ms.

The results show that compared with NC without GA, the proposed passivity-based NC using GA has shorter settling time when R changes. It has smaller value of $\triangle V$ when R is increased to 40 Ω. However, the NC without using GA has smaller value of IAE. The comparison results are described in Figure 13 and Table 7.

CONCLUSIONS

In this paper, the passivity-based neural control using genetic algorithm for a DC-DC boost power converter is proposed. The equilibrium point at origin of the plant (6) is asymptotically stable. The neural network performs the passivity-based control law. The simulation results of the passivity-based neural control using genetic algorithm and the results of the NC without using GA are done with Simulink in MATLAB.

The simulation results of the passivity-based neural control without using GA are done when the desired voltage V_d, the input voltage E and the load resistor R change. The results of the NC without using GA

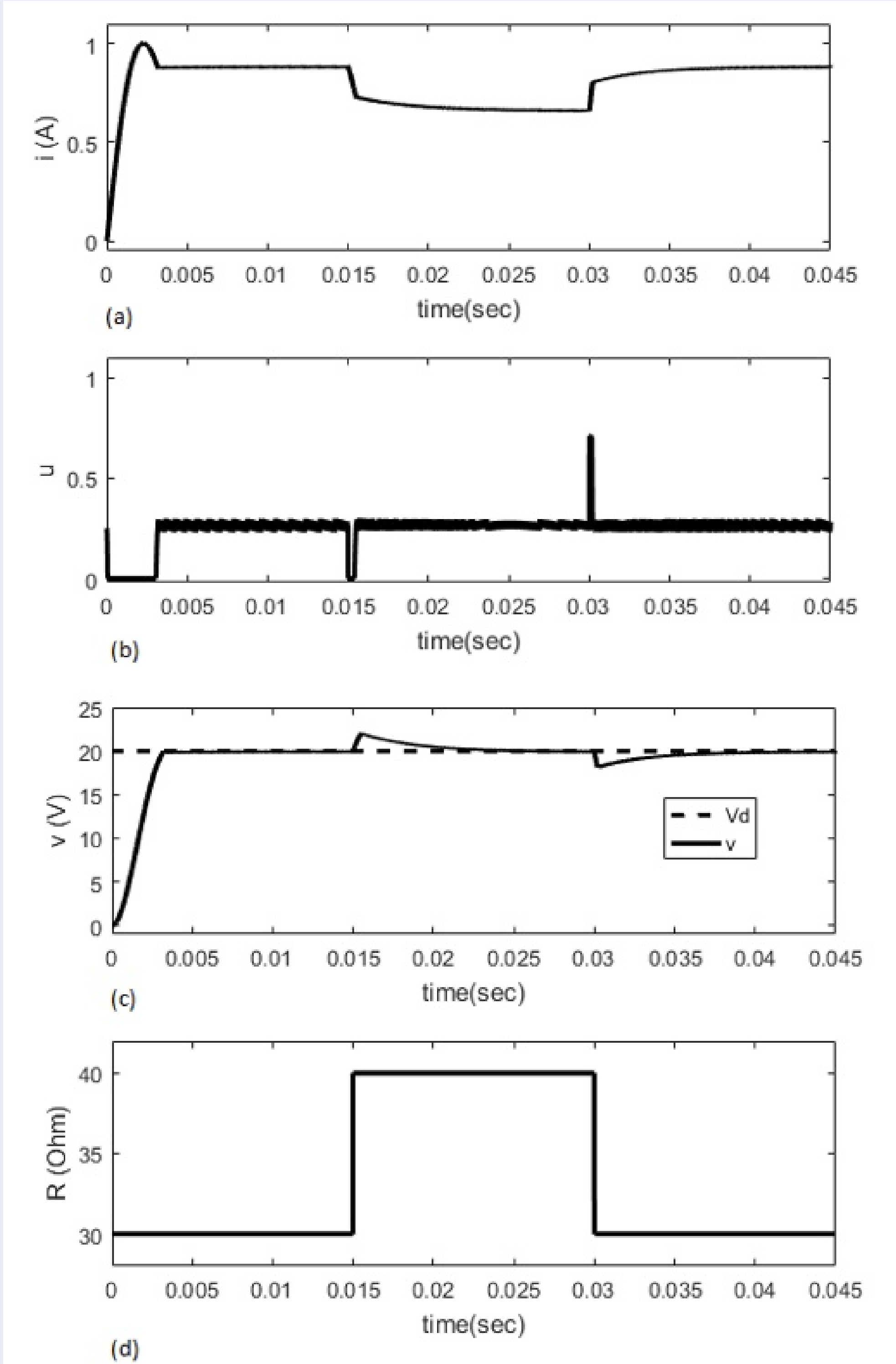

Figure 12: The results of the passivity-based NC using GA when R varies: (a) the inductor current i, (b) the control input u, (c) the capacitor voltage v and (d) R with q_1=1, q_2=1.

Table 7: The capacitor voltage v of the NC without GA and the passivity-based NC using GA with q_1=1, q_2=1 when R varies.

Controller	Increasing (+10 Ω)		Decreasing (-10 Ω)		IAE
	$\triangle V$ (V)	t_s (ms)	$\triangle V$ (V)	t_s (ms)	
NC without GA	2.10345	9.2	1.847	9.2	0.0478
Passivity-based NC using GA with q_1=1, q_2=1	2.022	2.8	1.873	2.8	0.0482

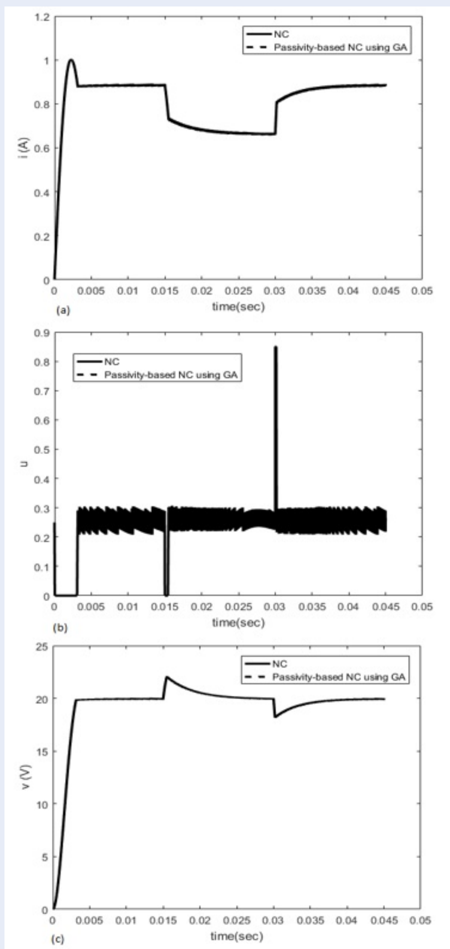

Figure 13: The results of NC without GA (continuous line) and the passivity-based NC using GA (discrete line) when R varies: (a) the inductor current i, (b) the control input u, and (c) the capacitor voltage v with q_1=1, q_2=1.

show that the capacitor voltage v is kept at the desired value. The results of the passivity-based NC using GA are performed when the input voltage E and the resistor R vary. The weights of the neural network are adjusted optimally using genetic algorithm with decimal encoder. The simulation results of the passivity-based neural control using GA show that the capacitor voltage v is kept at a desired value V_d. Genetic algorithm is integrated into a neural controller and adjusts optimally the weights of the neural network such as v_{11}, v_{21}, v_{31}, v_{12}, v_{22}, v_{32}, v_{13}, v_{23}, v_{33}, w_1, w_2 and w_3. The value of q_1 has influence to the inductor current i and decreases the settling time. The value of q_2 has influence to the capacitor voltage v and decreases the settling time.

The results show that compared with the neural control without GA, the proposed passivity-based neural control using GA has shorter settling time and smaller value of IAE when E changes. Moreover, the passivity-based NC using GA has smaller value of $\triangle V$ than the NC. The results show that compared with NC without GA, the proposed passivity-based NC using GA has shorter settling time when R changes. It has smaller value of $\triangle V$ when R is increased to 40 Ω. However, the NC without using GA has smaller value of IAE when R changes.

The paper has limitations such as the assumed circuit parameters. Future research will explore a practical real-time experiments.

ACKNOWLEDGEMENT

We acknowledge the support of time and facilities from Ho Chi Minh City University of Technology (HCMUT), VNU-HCM for this study.

ABBREVIATIONS

PBC - passivity-based control

GA - genetic algorithm

NC - neural control

COMPETING INTEREST

The authors agree with the manuscript of the paper and have no conflict. The paper has not been submitted in the other journal.

CONTRIBUTION OF THE AUTHORS

Hoai Nghia Duong is the corresponding author. He guides the research idea, gives suggestion to the paper so that Minh Ngoc Huynh corrects the paper. He gives the final agreement for the paper to submit.

Vinh Hao Nguyen is the author. He guides the research idea, gives suggestion to the paper so that Minh Ngoc Huynh corrects the paper.

Minh Ngoc Huynh is the first author. He writes the manuscript of the paper and does simulation. He corrects the paper according to Hoai Nghia Dương's and Vinh Hao Nguyen's suggestion and the reviewer'suggestion.

REFERENCES

1. Ortega R, Loria A, Nicklasson PJ, Sira-Ramirez H. Passivity-based control of Euler-Lagrange systems. Springer-Verlag; 1998. 543 p;Available from: https://doi.org/10.1007/978-1-4471-3603-3_2.
2. He W, Li S, Yang J, Wang Z. Incremental passivity-based control for DC-DC boost converter under time-varying disturbances via generalized proportional integral observer. J Power Electron. 2018;18(00):147-59;Available from: https://doi.org/10.1109/iecon.2016.7794073.
3. Cisneros R, Pirro M, Bergna G, Ortega R, Ippoliti G, Molinas M. Global tracking passivity-based PI control of bilinear systems and its applications to the boost and modular multilevel converters. IFAC-PapersOnLine. 2015;48(11):420-5;Available from: https://doi.org/10.1016/j.ifacol.2015.09.222.
4. Duong HN. Control of MIMO systems. Ho Chi Minh City: VNU Press; 2013. 199 p;.
5. Khalil HK. Nonlinear systems. 3rd ed. New Jersey: Prentice-Hall; 2002. 768 p;.
6. Huynh MN, Duong HN, Nguyen VH. Passivity-based control of bicycle robot. Sci Technol Dev J Eng Technol. 2022;5(2):1520-7;Available from: https://doi.org/10.32508/stdjet.v5i2.954.
7. Hayakawa T, Haddad WM, Bailey JM, Hovakimyan N. Passivity-based neural network adaptive output feedback for nonlinear nonnegative dynamical systems. Proc 42nd IEEE Int Conf Decis Control; 2003; Maui, HI, USA;Available from: https://doi.org/10.1109/CDC.2003.1271912.
8. Li W, Qin K, Chen B, Lin B, Shi M. Passivity-based distributed tracking control of uncertain agents via a neural network combined UDE. Neurocomputing. 2021;49:342-56;Available from: https://doi.org/10.1016/j.neucom.2021.03.008.
9. Norgaard M, Ravn O, Poulsen NK, Hansen LK. Neural networks for modelling and control of dynamic systems. Springer; 2000;.
10. Nguyen DM, Nguyen DT, Duong HN. Stabilize the inverted pendulum system using neural networks. J Comput Sci Cybern. 2010;26(3):245-52;.
11. Muthirayan D, Khargonekar PP. Memory augmented neural network adaptive controllers: performance and stability. IEEE Trans Autom Control. 2023;68(2):825-38;.
12. Escobar G, Ortega R, Sira-Ramires H, Vilain JP, Zein I. An experimental comparison of several nonlinear controllers for power converters. Proc 36th Conf Decis Control; 1997; California, USA. p. 227-8;.
13. Hassan MA, Li EP, Li X, Li T, Duan C, Chi S. Adaptive passivity-based control of DC–DC buck power converter with constant power load in DC microgrid systems. IEEE J Emerg Sel Top Power Electron. 2019;7(3):2029-40;.
14. Mitchell M. An introduction to genetic algorithms. MIT Press; 1999;.
15. Tang KS, Chan CY, Man KF, Kwong S. Genetic structure for neural network topology and weights optimization. Proc 1st IEE/IEEE Int Conf GA's Eng Syst Innov Appl; 1995; Sheffield, U.K. p. 250-5;.
16. Nizami TK, Chakravarty A. Neural network integrated adaptive backstepping control of DC-DC boost converter. IFAC-PapersOnLine. 2020;53(1):549-54;Available from: https://doi.org/10.1016/j.ifacol.2020.06.092.
17. Aguila-Leon J, Chinas-Palacinos CD, Vargas-Salvado C, Hurtado-Perez E, Garcia EXM. Optimal PID parameters tuning for a DC-DC boost converter: a performance comparative using grey wolf optimizer, particle swarm optimization and genetic algorithm. 2020 IEEE Conf Technol Sustain (SusTech); 2020. p. 1-6;Available from: https://doi.org/10.1109/SusTech47890.2020.9150507.
18. Mohammedi M, Kraa O, Becherif M, Aboubou A, Ayad MY, Bahri M. Fuzzy logic and passivity-based controller applied to electric vehicle using fuel cell and supercapacitors hybrid source. Int Conf Technol Mater Renew Energy, Environ Sustain (TMREES14); 2014. Energy Procedia 50:619-26;.
19. Huynh MN, Duong HN, Nguyen VH. Passivity-based control using genetic algorithm for a DC-DC boost power converter. Sci Technol Dev J Eng Technol. 2023;6(2):1891-905;Available from: https://doi.org/10.32508/stdjet.v6i2.1053.
20. Huynh MN, Duong HN, Nguyen VH. A passivity-based control combined with sliding mode control for a DC-DC boost power converter. J Robot Control. 2023;4(6):780-90;Available from: https://doi.org/10.18196/jrc.v4i6.20071.
21. Wu J, Lu Y. Adaptive backstepping sliding mode control for boost converter with constant power load. IEEE Access. 2019;7:50797-807;Available from: https://doi.org/10.1109/ACCESS.2019.2910936.

Tạp chí Phát triển Khoa học và Công nghệ – Engineering and Technology 2025, ():1-1

Open Access Full Text Article

Bài nghiên cứu

Điều khiển mạng nơron dựa vào tính thụ động dùng giải thuật di truyền cho bộ biến đổi công suất boost DC-DC

Minh Ngọc Huỳnh[1,2], Hoài Nghĩa Dương[3,*], Vĩnh Hảo Nguyễn[1]

TÓM TẮT

Trong bài báo này, điều khiển mạng nơron dựa vào tính thụ động dùng giải thuật di truyền cho bộ biến đổi công suất boost DC-DC được đề nghị. Ngõ ra của bộ biến đổi công suất boost DC-DC là dòng điện cuộn cảm. Ngõ vào điều khiển là tỉ lệ nhiệm vụ. Sử dụng phép biến đổi tọa độ của các biến trạng thái và tín hiệu điều khiển, bộ biến đổi công suất boost DC-DC là thụ động. Hệ mới là quan sát được trạng thái 0 và điểm cân bằng ở gốc tọa độ của hệ này là ổn định tiệm cận. Mạng nơron thực hiện luật điều khiển dựa vào tính thụ động. Mục tiêu là điện áp trên tụ điện bằng với điện áp mong muốn. Mạng nơron có ba lớp: lớp ngõ vào, lớp ẩn và lớp ngõ ra. Hàm tác động của lớp ẩn là tan-hyperbol và hàm tác động của lớp ngõ ra là tuyến tính. Trọng số của mạng nơron được chỉnh tối ưu bằng giải thuật di truyền dùng mã hóa thập phân. Kết quả mô phỏng được thực hiện bằng Simulink trong MATLAB. Kết quả mô phỏng của điều khiển mạng nơron dựa vào tính thụ động không dùng giải thuật di truyền chứng tỏ rằng điện áp trên tụ điện được giữ ổn định tại điện áp mong muốn khi điện áp mong muốn, điện áp ngõ vào và điện trở tải thay đổi. Kết quả của điều khiển mạng nơron dựa vào tính thụ động dùng giải thuật di truyền chứng tỏ rằng điện áp trên tụ điện được giữ ổn định tại điện áp mong muốn khi điện áp ngõ vào và điện trở tải thay đổi. Hơn nữa, kết quả mô phỏng của điều khiển mạng nơron dựa vào tính thụ động dùng giải thuật di truyền có chất lượng tốt hơn như là thời gian quá độ ngắn hơn và giá trị IAE (integral absolute error of the desired voltage and the capacitor voltage) nhỏ hơn kết quả của điều khiển mạng nơron khi điện áp ngõ vào thay đổi. Cuối cùng, kết quả mô phỏng chứng tỏ rằng điều khiển mạng nơron dựa vào tính thụ động dùng giải thuật di truyền có thời gian quá độ ngắn hơn điều khiển mạng nơron khi điện trở tải thay đổi.

Từ khoá: bộ biến đổi công suất boost DC-DC, điều khiển mạng nơron, điều khiển dựa vào tính thụ động, giải thuật di truyền

[1]*Trường Đại học Bách khoa – ĐHQG-HCM, Việt Nam*

[2]*Trường Đại học Công nghiệp TP. HCM*

[3]*Đại học Quốc tế Miền Đông*

Liên hệ

Hoài Nghĩa Dương, Đại học Quốc tế Miền Đông

Email: nghia.duong@eiu.edu.vn

Lịch sử

- Ngày nhận: 16-1-2024
- Ngày sửa đổi: 31-8-2024
- Ngày chấp nhận: 22-10-2024
- Ngày đăng:

DOI :

Trích dẫn bài báo này: Huỳnh M N, Dương H N, Nguyễn V H. **Điều khiển mạng nơron dựa vào tính thụ động dùng giải thuật di truyền cho bộ biến đổi công suất boost DC-DC**. *Sci. Tech. Dev. J. - Eng. Tech.* 2025; ():1-1.